ISSN 1547-4771, Physics of Particles and Nuclei Letters, 2022, Vol. 19, No. 6, pp. 717–723. © Pleiades Publishing, Ltd., 2022.
Russian Text © The Author(s), 2022, published in Pis'ma v Zhurnal Fizika Elementarnykh Chastits i Atomnogo Yadra, 2022.

PHYSICS OF ELEMENTARY PARTICLES AND ATOMIC NUCLEI. EXPERIMENT

Determination of Carbon Concentration in Soil Using the Tagged Neutron Method

V. Yu. Alexakhin[a, b,*], E. A. Razinkov[a, **], Yu. N. Rogov[a, b, *], A. B. Sadovsky[a, b, ****], M. G. Sapozhnikov[a, b, *****], I. D. Dashkov[b, ******], D. N. Grozdanov[b, c, *******], Yu. N. Kopach[b, ********], V. R. Skoy[b, *********], and N. A. Fedorov[b, **********]**

[a] *OOO Diamant, Dubna, 141980 Russia*

[b] *Joint Institute for Nuclear Research, Dubna, 141980 Russia*

[c] *Institute for Nuclear Research and Nuclear Energy of the Bulgarian Academy of Science, Sofia, 1784 Bulgaria*

**e-mail: alexakhin@jinr.ru*

***e-mail: erazinkov@diamant-sk.ru*

****e-mail: yrogov@diamant-sk.ru*

*****e-mail: sadovski@jinr.ru*

******e-mail: sapozhnikov@jinr.ru*

*******e-mail: daschkov.id15@physics.msu.ru*

********e-mail: dimitar@nf.jinr.ru*

*********e-mail: kopatch@nf.jinr.ru*

**********e-mail: skoy@nf.jinr.ru*

***********e-mail: na.fedorov@physics.msu.ru*

Received March 16, 2021; revised April 8, 2022; accepted April 8, 2022

Abstract—The results of determining the mass concentration of carbon in soil are discussed. The measurements were made on a facility operating according to the tagged neutron method, which consists of irradiating samples with 14 MeV fast neutrons and detecting the characteristic spectra of gamma rays from inelastic neutron scattering at specific time ranges between neutron emission and arrival of the γ-quantum signal. The values of the accuracies of the measurements have been estimated, the standard deviation of the repeated measurements for concentrations of carbon of 1–3% was $\sigma_r = 0.14\%$, the convergence to the calculated values was $\sigma_r = 0.2\%$.

DOI: 10.1134/S1547477122060024

INTRODUCTION

With climate change and rising atmospheric CO_2 attention is being paid to soil organic carbon sequestration and the role of soil as a carbon sink. Carbon sequestration in plants and soil systems is known to provide an opportunity to mitigate the greenhouse effect, with the relationship between carbon storage in soils and carbon fixation in natural and anthropogenic vegetation remains one of the least studied problems.

Typically, the carbon concentration in soil is determined by chemical methods "dry" or "wet" combustion of the sample [1]. For "wet" combustion of a sample (the Tyurin method) 20% relative error of the results of the analysis (at the confidence level of $P = 0.95$) is allowed at a mass fraction of organic matter up to 3% [1]. The method of dry combustion of the sample is much more accurate, but requires a lot of time, as one determination requires 2.5–3 h [2]. In addition, it requires substantial sample preparation.

Recently, to analyze the elemental composition of soil, the methods of laser (LIBS) and infrared (NIRS) spectroscopy [3] is suggested. The main disadvantage of these methods is that they only give an idea of the elemental composition of small areas of the surface soil layer, from 0.1 to 1 cm deep.

These drawbacks are deprived of the use of neutron methods of analysis, in particular, the method of tagged neutrons [4, 5].

The Tagged Neutron Method (TNM) consists of irradiating the object under study by fast neutrons with an energy of 14.1 MeV (Fig. 1), which are produced in a binary reaction:

$$d + {}^3\mathrm{H} \rightarrow {}^4\mathrm{He} + n. \quad (1)$$

In this reaction, the neutron and the α-particle (^{4}He nucleus) fly practically in opposite directions. Therefore, by registering the α-particle accompanying the neutron, it is possible to determine the direction

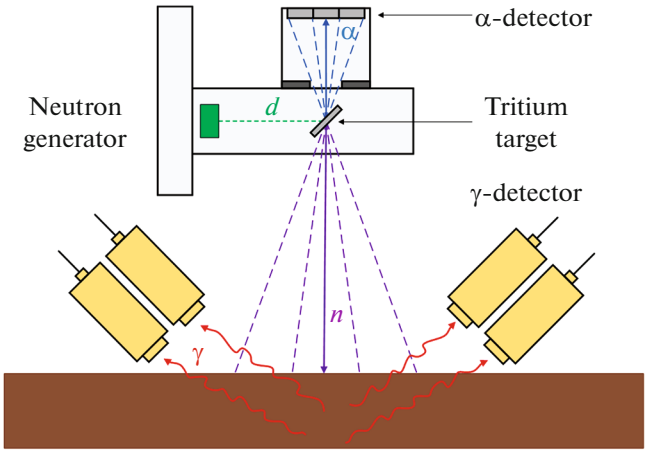

Fig. 1. General scheme of the tagged neutron method.

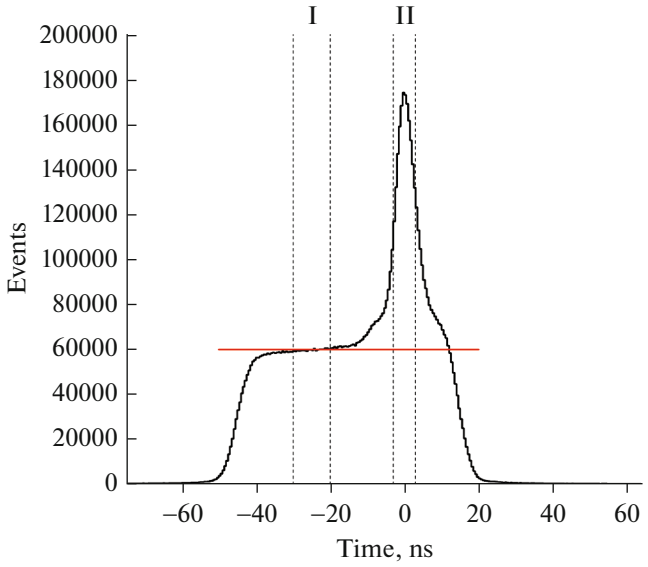

Fig. 2. Time distribution in coincidence window of 60 ns; the dotted line on the left shows the region of the random coincidence plateau (the random coincidence plateau is shown in red), 10 ns wide, which is used as a background; the dotted line on the right highlights the peak region 6 ns wide.

and time of the neutron escape. This procedure is called neutron tagging. When tagged neutrons enter the test object they induce nuclear reactions whereby the excitation of the nuclear products is removed by the emission of γ-quanta with an energy spectrum characteristic for each chemical element. Registration of characteristic γ-radiation is performed by γ-detectors in coincidence with the α-detector signal. This makes it possible to separate γ-quanta that come from interactions with the investigated object, from background radiation that is not related to the spatial region under study. This is the important difference between TNM and other known methods of neutron analysis—it does not simply determine the energy spectrum in the entire region of the inspection, but differentiates this information by individual spatial elements of the sample.

At present, various detection systems have been developed on the basis of TNM to determine the presence of explosives in the objects of control up to the sea containers [6–8]. Analyzers have been developed both for determining the elemental composition of individual samples in the field conditions [9] and for the analysis of sinter or phosphate ores on a conveyor. The TNM has been successfully applied to detect diamonds within kimberlite rock without crushing it [10–12].

DESCRIPTION OF THE FACILITY

The measurements were carried out on the prototype of facility for determination of elemental composition of carbon in soil AGP-C. It consisted of an ING-27 portable neutron generator with built-in 9-pixel α-detector, a system of 6 γ-detectors on the basis of BGO crystals, data acquisition system, power supply for detectors and neutron generator.

ING-27 portable neutron generator emits neutrons with energy 14.1MeV. The measurements were taken at neutron generator intensity $I = 2.5 \times 10^7$ s^{-1}. Built-in silicon α-detector was a 3 × 3 matrix with a pixel size of 10 × 10 mm, located at a distance of 62 mm from the tritium target.

To register γ-rays arising during irradiation of the soil with a beam of fast tagged neutrons, six γ-detectors based on BGO crystals 76 mm in diameter and 65 mm thick were used.

The detectors used Hamamatsu photomultiplier tubes of R6233. These detectors have an optimum cost/performance ratio and have proven themselves in TNM facilities. At 4.44 MeV, the energy resolution of the entire detector system was $\Gamma_E = 4.42 \pm 0.14\%$, and the time resolution of the system of (α-γ)-coincidences, averaged over the entire set of γ-detectors, was $\Gamma_t = 4.82 \pm 0.12$ ns.

Figure 2 shows a typical time distribution of events recorded with the detector during irradiation of the sample with the ING-27 neutron generator. The spectrum was collected in a window of coincidences of 60 ns width, which opens at the moment of α-particle arrival.

It can be seen that during this time, among other things, records events from the interaction of untagged neutrons with surrounding objects, they give a plateau of random coincidences (the area of the plateau, which used as the background is marked I). A pronounced peak is formed by γ-quanta from the of the research object (II), the amplitude of the peak is several times greater than the amplitude of the plateau of random coincidences.

On Fig. 3 shows the energy spectrum of the shelf of random coincidences (region I in Fig. 2) and the spectrum formed by γ-quanta from the object under study (region II in Fig. 2). The energy calibration was carried out using reference characteristic peaks: Fe (847 keV), Fe (1238 keV), C (4438 keV), O (6129 keV).

MEASUREMENT TECHNIQUE

Measurements were performed without any preliminary preparation and processing samples. The spectra were processed according to the technique that was described in detail in [13, 14].

The gamma-spectrum of each sample was decomposed into separate components by fitting it with the sum of the reference γ-spectra from 9 elements, which were measured on the same experimental setup in advance. The reference elements, necessary to describe the soil spectrum were Al, C, Ca, Fe, Mg, Na, O, P, and Si.

The energy spectrum of γ-rays from irradiation of the sample with fast neutrons with energy of 14 MeV is represented as a sum of spectra of individual γ-lines, continuum and background spectra:

$$F(E) = \sum_j N_j \left(\sum_{i=1}^{i=n_j} \sigma_{ij}(E) P_{ij}(E) + R_j^{\mathrm{Cont}} F_j^{\mathrm{Cont}}(E) \right) + BG(E), \quad (2)$$

where N_j is the parameter determining the content of element j in the sample, and this is proportional to the number of atoms of the element in the sample and is the same for each γ-line with the number i of element j;

n_i is the number of γ-lines i of element j;

$\sigma_{ij}(E)$ is the cross-section of the production of γ-rays with energy E, corresponding to the gamma-line i, in the interaction of a neutron with element j;

P_{ij} is the response function of the γ-detector, corresponding to the γ-line i of element j;

$F_j^{\mathrm{Cont}}(E)$ is the amplitude of the spectrum of the continuum which is observed at high excitation energies for practically all nuclei except the lightest ones;

R_j^{Cont} is the normalization factor for the continuum spectrum;

$BG(E) = A\exp(-BE)$ is the background function, A and B are the fitting parameters.

To obtain the characteristic γ-spectra of the reagents of main chemical elements and of corresponding oxides (Al_2O_3, CaO, Fe_2O_3, MgO, Na_2CO_3, P_2O_3, SiO_2) with a purity not lower than "pure", as well as a carbon plate and water were used. The detailed characteristics of the reagents are given in Table 1.

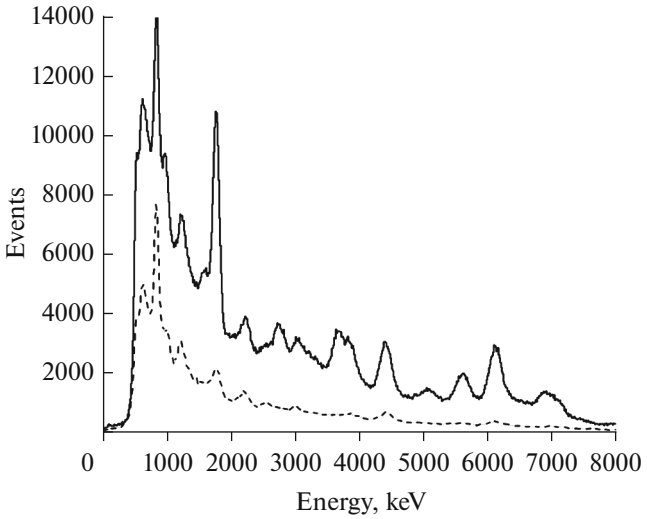

Fig. 3. The energy spectrum of γ-quanta corresponding to the time domain I in Fig. 2, is shown by a dotted line; the energy spectrum of γ-quanta corresponding to the time domain II in Fig. 2 is shown as a solid line.

Each reagent was measured for 90 min. Figure 4 shows the energy spectra of γ-quanta for the oxides used in the analysis.

On Fig. 5 shows a typical energy spectrum of gamma quanta of a soil sample. This spectrum is obtained by subtracting the energy spectrum of random coincidences corresponding to region of the time spectrum II from the energy spectrum corresponding to region of the time spectrum I (see Figs. 2 and 3). Points with errors show experimental data. Different colors show the contributions from the energy spectra of individual elements. The dark-blue line shows the total contribution from all elements. It can be seen that the main contributions to the soil spectrum come from oxygen (blue line), silicon (green line), and carbon (red line). The contributions from all other elements present in the fit turned out to be zero.

We can also clearly see how small the contribution of carbon to the overall spectrum is. Therefore, the

Table 1. List of reagents and their characteristics

No.	Sample name	Purity, %	Weight, kg
1	Al_2O_3	Pure for analysis (97.0)	2.0
2	CaO	Pure (96.0)	2.0
3	Fe_2O_3	Pure (95.0)	2.0
4	MgO	Pure for analysis (98.0)	2.0
5	Na_2CO_3	Pure (99.8)	1.0
6	P_2O_5	Pure (98.0)	2.5
7	SiO_2	Pure (96.0)	2.0
8	C^{12}		2.0
9	H_2O		2.0

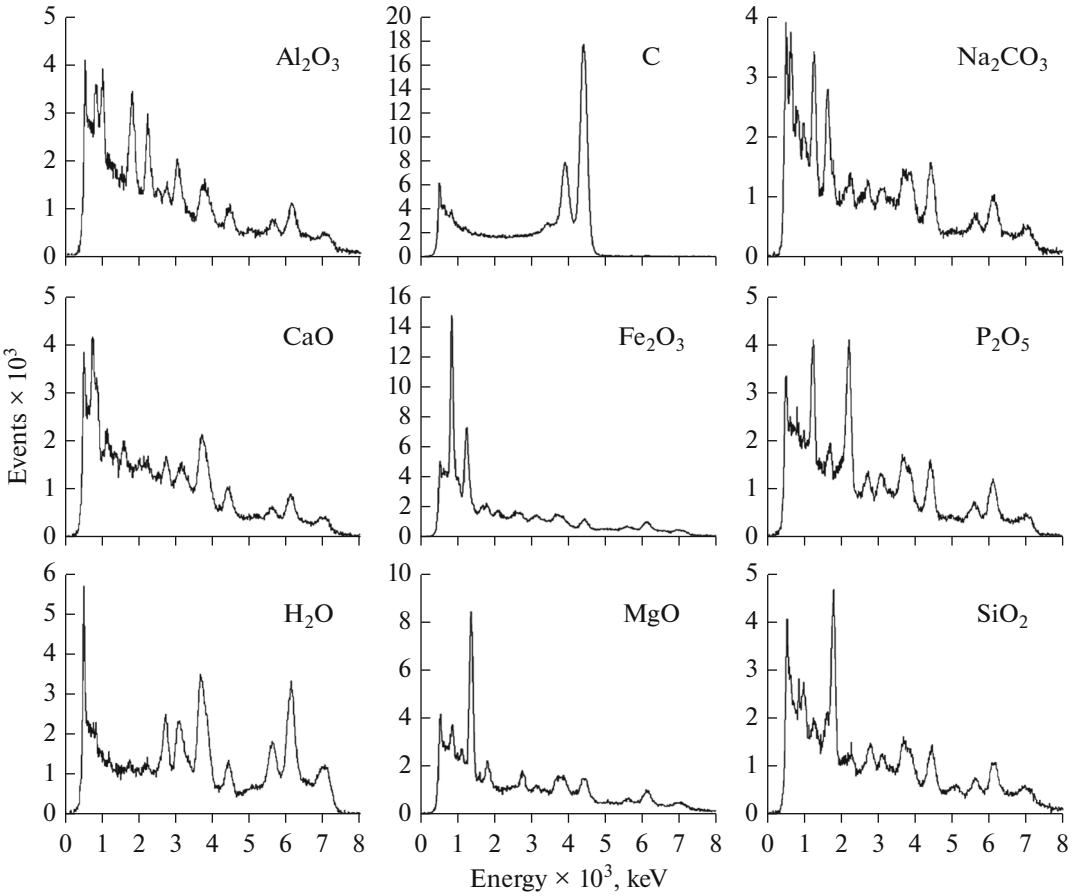

Fig. 4. Energy spectra of γ-quanta from the oxides of basic elements.

task of determining the carbon concentration with good accuracy is far from trivial. The carbon spectrum obtained in the reaction $^{12}C(n, n'\gamma)^{12}C^*$ is quite simple (see Fig. 4). In it dominates the line with an energy of 4.44 MeV. However, it should be taken into account that in interacting with oxygen nuclei, fast neutrons can initiate the reaction $^{16}O(n, n'\alpha)^{12}C^*$ through the emission of a γ-quantum with energy 4.44 MeV. The corresponding peak is clearly visible in the spectrum of oxygen (see Fig. 4). Also in spectrum of silicon in the region of 4.50 MeV a peak can be seen from γ-quanta produced by the removal of ^{28}Si in reaction $^{28}Si(n,n'\gamma)^{28}Si^*$. It is shown in the inset in Fig. 5, where the part of the soil gamma ray spectrum in the region of 3.6–5.2 MeV. It can be seen that the observed peak at 4.4 MeV consists of contributions from different reactions, so directly linking the number of events under the peak with the carbon concentration in the soil is impossible.

MEASUREMENT OF CALIBRATION SAMPLES

The most important task of soil elemental analysis is the construction of a reliable calibration curve. To do this, it is necessary to measure a certain number of samples with different concentrations and compare the TNM data to the results of chemical analysis. The task is rather complicated, especially since it presupposes the use of an installation for the analysis of different soils with considerably different elemental compositions. In our work we applied a calibration procedure, which used measurements of samples made up of silica sand and sugar sand in different proportions. The mass of each sample was 30 kg, the sugar content was chosen so that the mass fraction of carbon in the sample varied from 0 to 10%. Measurements were carried out in the mode 3 × 30 min. The average of processing of each of three measurements was taken as a result.

Figure 6 shows the results of measurements of calibration samples as well as the calibration dependence (red line).

The obtained results were well approximated by a simple linear function with the following parameters:

$$Y = (1.03 \pm 0.03)C_{\text{raw}} - (0.31 \pm 0.12), \qquad (3)$$

where C_{raw} is the result of the measurements of AGP-C facility, Y is the mass concentration of carbon in the sample.

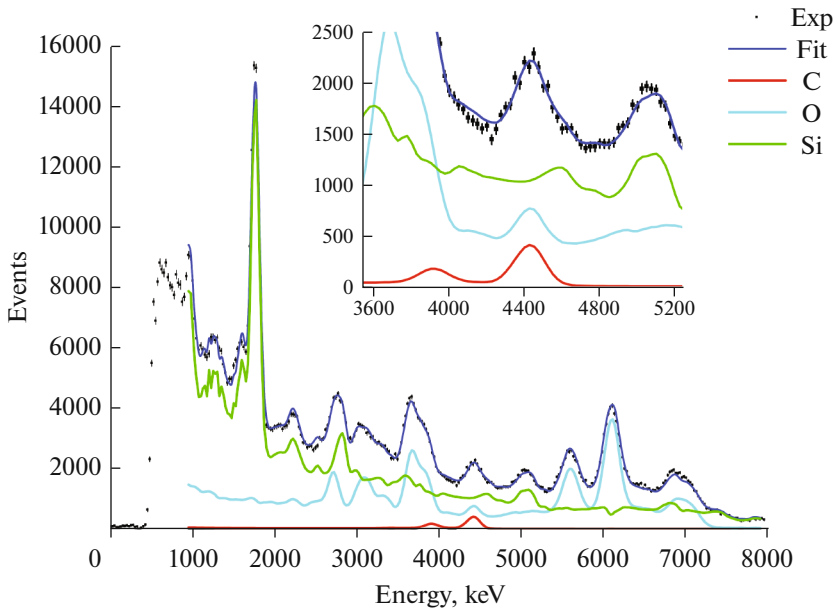

Fig. 5. Energy spectrum of γ-quanta of a soil sample. Points with errors show experimental data. Different colors show the contributions from the energy spectra of individual elements. The blue line shows the contribution from oxygen, the green dashed line shows the contribution from silicon, and the red line shows the contribution from carbon. The dark-blue line shows the total contribution from all elements.

Table 2 shows the values of carbon concentration with the corresponding errors after conversion according to (3). The correlation plot of the measurement results after calibration is shown in Fig. 7.

The scatter of calibration data (convergence with the calculated values) is characterized by the standard deviation (RMS):

$$\sigma_r = \sqrt{\frac{\sum_i (X_i - Y_i)^2}{n}} = 0.2\% \,, \qquad (4)$$

where n is the number of samples, X is the value of mass concentration measured by AGP-C for sample i, Y is the value of mass concentration according to calculations for sample i.

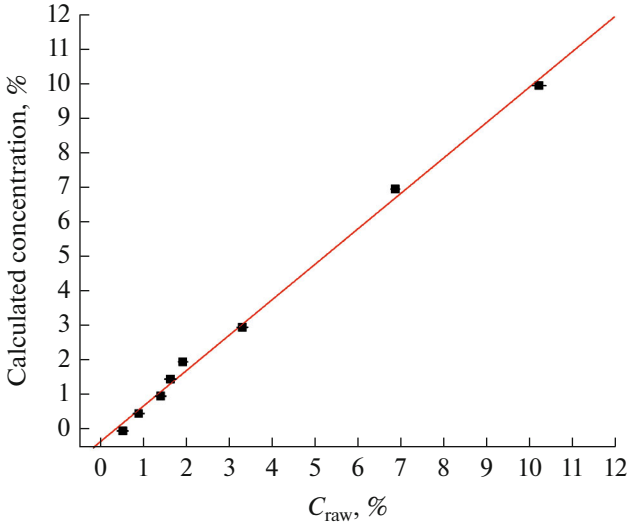

Fig. 6. Measurement results of calibration samples. The abscissa axis shows the results of measurements of the carbon concentration by the AGP-C facility, and the calculated values are plotted along the ordinate axis. The red line shows the calibration function. The marker size is greater than the measurement error value.

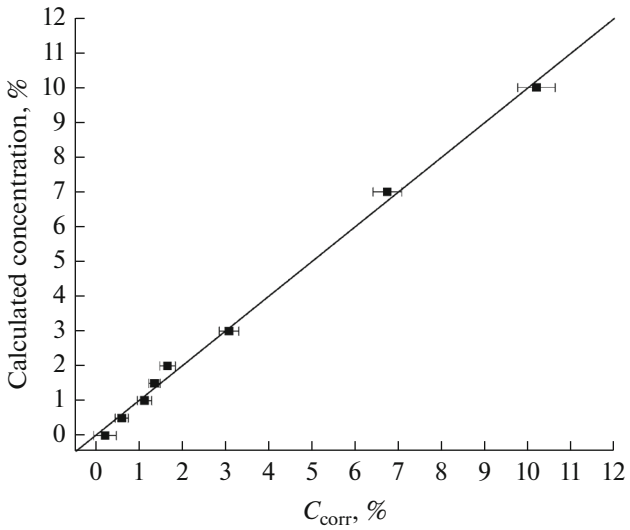

Fig. 7. Measurement results after calibration. The abscissa axis shows the results of measurements of the mass concentration of carbon after calibration, and the calculated values are plotted along the ordinate axis. The black line shows the diagonal of equal values.

Table 2. Mass fractions of carbon according to measurements of calibration samples

Concentration of C, %	C_{corr}, %	$\pm\Delta_{corr}$, %
0	0.22	0.26
0.5	0.60	0.15
1.0	1.13	0.17
1.5	1.36	0.13
2.0	1.66	0.18
3.0	3.09	0.22
7.0	6.75	0.33
10.0	10.19	0.43

Table 3. Mass concentrations of carbon according to measurements of calibration samples

	Averaged concentration, %	σ_r, %	σ_r^{rel}, %
C	3.30	0.16	4.7
	1.70	0.12	6.9
O	52.01	0.45	0.9
	52.62	0.65	1.2
Si	44.65	0.29	0.6
	39.23	0.63	1.6

To determine the capabilities of the equipment, the measurement accuracy in terms of repeatability was determined. To do this, two samples were measured 12 times for 30 min without changing the setup configuration and the position of the samples in space.

Table 3 shows the absolute σ_r and relative σ_r^{rel} RMS of repeatability:

$$\sigma_r = \sqrt{\frac{\sum_i (C_i - C)^2}{n-1}}, \quad (5)$$

$$\sigma_r^{rel} = \frac{\sigma_r}{C} \times 100\%, \quad (6)$$

where n is the number of measurements, C is the average value of element mass concentration for all measurements, C_i is the element mass concentration in the i-measurement.

Thus, the averaged absolute error of repeated measurements of the mass concentration of carbon in the soil turns out to be 0.14%, for silicon it is 0.46%, for oxygen it is 0.55%.

CONCLUSIONS

The capabilities of the facility for determining the elemental composition of soil using the method of tagged neutrons are estimated. A procedure for calibration of the facility has been developed. The measurements of soil samples and calibration samples were performed. For mass concentration of carbon, absolute RMS values of repeated measurements $\sigma_r = 0.14\%$ were obtained for carbon concentrations of 1–3%. Convergence with the calculated values was $\sigma_r = 0.2\%$.

ACKNOWLEDGMENTS

The authors are grateful to the employees of Diamant, E.I. Andreev, E.V. Zubarev, V.K. Rodionov, and O.G. Tarasov, who participated in the creation and testing of the facility and D.N. Borisov (JINR) for his help in preparing the samples.

CONFLICT OF INTEREST

The authors declare that they have no conflicts of interest.

REFERENCES

1. GOST (State Standard) 26213–91: Methods for determining organic matter.
2. A Practical Guide to Soil Chemistry. https://studfile.net/preview/2465162/page:40/.
3. D. Milori, A. Segnini, W. T. L. da Silva, A. Posadas, V. Mares, R. Quiroz, and L. Martin-Neto, "Emerging techniques for soil carbon measurements," in *Climate Change Mitigation and Agriculture,* Ed. by E. Wollenberg (2011), Vol. 2.
4. G. Yakubova, L. Wielopolski, A. Kavetskiy, A. Torbert, and S. Prior, "Field testing a mobile inelastic neutron scattering system to measure soil carbon," Soil Sci. **179**, 529 (2014).
5. V. Valkovic, *14 MeV Neutrons: Physics and Applications* (CRC, Boca Raton, 2015), Vol. 94, p. 262.
6. V. M. Bystritsky, V. V. Gerasimov, V. G. Kadyshevsky, A. P. Kobzev, A. A. Nozdrin, Y. N. Rogov, V. L. Rapatsky, A. B. Sadovsky, A. V. Salamatin, M. G. Sapozhnikov, A. N. Sissakian, I. V. Slepnev, V. M. Slepnev, V. A. Utkin, N. I. Zamyatin, et al., "DViN-stationary setup for identification of explosives," Phys. Part. Nucl. Lett. **5**, 441–446 (2008).
7. V. M. Bystritsky, N. I. Zamyatin, E. V. Zubarev, V. L. Rapatsky, Y. N. Rogov, I. V. Romanov, A. B. Sadovsky, A. V. Salamatin, M. G. Sapozhnikov, M. V. Safonov, V. M. Slepnev, and A. V. Philipov, "Stationary setup for identifying explosives using the tagged neutron method," Phys. Part. Nucl. Lett. **10**, 442–446 (2013).
8. S. Pesente, G. Nebbia, G. Viesti, F. Daniele, D. Fabris, M. Lunardon, S. Moretto, K. Nad, D. Sudac, and V. Valkovic, "Progress in tagged neutron beams for cargo inspections," Nucl. Instrum. Methods Phys. Res., Sect. B **261**, 268–271.
9. I. Bolshakov, M. Kolesnik, M. Sorokin, V. Kremenets, E. Razinkov, Y. Rogov, and M. Sapozhnikov, "Application of tagged neutron method for element analysis of phosphorus ore," Int. J. Mineral Process. Extract. Metall. **5**, 54–59 (2020).
10. V. Y. Aleksakhin, V. M. Bystritsky, N. I. Zamyatin, E. V. Zubarev, A. V. Krasnoperov, V. L. Rapatsky,

Y. N. Rogov, A. B. Sadovsky, A. V. Salamatin, R. A. Salmin, M. G. Sapozhnikov, V. M. Slepnev, S. V. Khabarov, E. A. Razinkov, O. G. Tarasov, and G. M. Nikitin, "Detection of diamonds in kimberlite by the tagged neutron method," Nucl. Instrum. Methods Phys. Res., Sect. A **785**, 9–13 (2015).

11. V. M. Bystritsky, G. M. Nikitin, Y. N. Rogov, A. B. Sadovsky, and M. G. Sapozhnikov, "Application of the tagged neutron method for diamonds detection in kimberlite," in *Proceedings of the International Mineral Processing Congress IMPC 2018*.
12. Y. N. Rogov, V. Kremenets, M. Sapozhnikov, and M. Sebele, "Application of tagged neutron method for detecting diamonds in kimberlite," Instruments **4**, 33 (2020).
13. V. Yu. Aleksakhin, V. M. Bystritskii, N. I. Zamyatin, E. V. Zubarev, A. V. Krasnoperov, V. L. Rapatskii, A. V. Rogachev, Yu. N. Rogov, A. B. Sadovskii, R. A. Salmin, M. G. Sapozhnikov, V. M. Slepnev, S. V. Khabarov, E. A. Razinkov, O. E. Tarasov, E. V. Sklyarov, N. N. Ukhova, and A. V. Lavrenchuk, "Assessment of the possibility of determining the elemental composition of rocks using the tagged neutron method," Preprint OIYaI No. 14-2015-52 (Dubna, 2015).
14. V. Y. Aleoakhin, V. M. Bystritsky, N. I. Zamyatin, E. V. Zubarev, A. V. Krasnoperov, V. L. Rapatsky, A. V. Rogachev, Y. N. Rogov, A. B. Sadovsky, R. A. Salmin, M. G. Sapozhnikov, V. M. Slepnev, S. V. Khabarov, E. A. Razinkov, O. G. Tarasov, E. V. Sklyarov, and A. V. Lavrenchuk, "Determination of the elemental composition of geological rocks and minerals by the method of tagged neutrons," in *Proceedings of the 23rd International Seminar on Interaction of Neutrons with Nuclei ISINN-23, Dubna, May 25–29, 2015*.